Using Abaqus/Explicit to model polymeric thin-film mechanical property changes due to embossing

Colmar Wocke

Dow Chemical, Wolleraustrasse 15-17, CH-8807 Freienbach, Switzerland

Abstract: *Embossing of polymeric films destined for usage in the personal care marketplace is an industrial process that produces a very fine pattern, barely discernible to the naked eye, yet has a significant influence on some market-driven properties; more bulk, a soft and smooth touch, reduced crinkling noise and lower gloss. However this comes at a cost to the mechanical properties such as stiffness and ultimate strength capability. Since the feature size of the embossing pattern is so small, it is difficult to obtain all the information from an experiment alone, making the Finite Element Method an ideal analytical tool to help gain additional insight into the effects of some of the design and process parameters. The paper discusses the computational approach, presents results of simulations performed in Abaqus/Explicit for an example 16 micron film and compares to experimentally measured values.*

Keywords: *Constitutive Model, Damage, Experimental Verification, Forming, Fracture, Heat Transfer, Plasticity, Polymer, Residual Stress, Springback, Thermal Stress, Tissue, Visualization.*

1. Introduction

Off-line cold embossing is a stand-alone unit operation that consists of unwinding previously blown and slit film, contact-heating it with a roll to a semi-molten state, passing it through a cold nip formed between a hard engraving roll in contact with a soft backup roll and re-winding the structured film as schematically shown in Figure 1. Embossing produces a very fine pattern on the film, which is barely discernible to the naked eye, yet has significant influence on its properties. Compared to the flat precursor film, the embossed film has more bulk, has a soft and smooth touch, and reduced noise – all much desired in hygiene tissue films used for diapers. Furthermore the film has very low gloss, and features a reduced modulus, along with improved dart impact strength.

In addition to the analysis reported in [Kamal, 1988], these authors have been involved in additional studies along the same lines [Kamal, 1985; Kamal, 1992] that together form a good basis for the analysis conducted here. Since the time of these investigations, the capability to analyze these kinds of problems, using commercially-available Finite Element programs, has advanced significantly [Nagarajan]; Dow has chosen to analyze the problem using the capabilities available within Abaqus/Explicit from SIMULIA. Our analysis does not cover material structure-property relationships or in-depth analysis of toughening effects; we perform an analysis using the measured material test data, along different axes, as a basis for our input to the program. It is unusual to have all the test data required (even for fairly basic material models) since the material flows readily at the embossing temperature which makes testing very difficult; the complete material data required to be input has thus been synthesized from measured data together with some additional theoretical considerations and reasonable estimates.

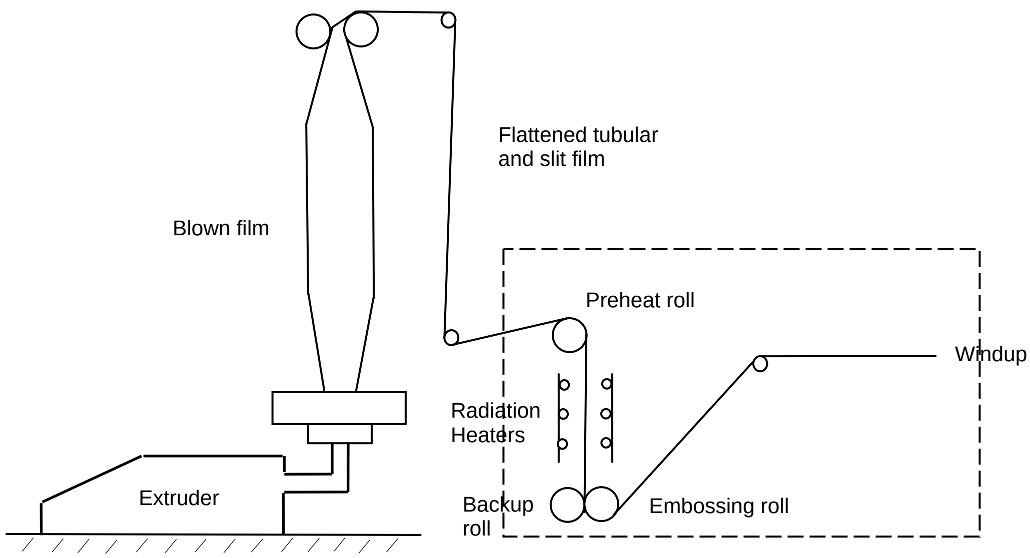

Figure 1 Film embossing schematic, showing Abaqus analysis window [from Kamal, 1988].

The primary mechanical property variable of interest is the alteration of the stiffness of the thin film due to the embossed pattern. However, an explicit Finite Element analysis offers the prospects of being able to conduct a **failure analysis** of the embossed film and to present this in animated form to the requestor of the analysis.

Concisely stated, the problem statement is:

Is it possible to successfully model

1. The Process, to investigate various effects on the material.
2. The Geometric Effect.

and in so-doing, determine the final properties of the embossed film in sufficient detail to help with some film embossing design decisions?

This paper covers some details associated with the parametric mesh generation of the embossing pattern, the material tests conducted, selection of a suitable material model from the library available in Abaqus and the synthesis of the required information in order to have sufficient information available for the analysis.

2. Background information to the analysis.

The blown film, before it enters the heating and embossing phase, is already oriented and its mechanical properties show a directional dependency. Subsequent operations may relax (heating and cooling) some of this oriented structure, introduce new orientations (mechanical embossing) and perhaps add internal damage or remove internal constraints to the material (heating and cooling and mechanical embossing). One can, for example, see some fairly sharp edges after the embossing process in the cross-sectional cut shown in Figure 2.

The **modeling** of any re-orientation, removal of internal constraints and damage effects within the material structure as a consequence of **thermal** treatment is not within the scope of this analysis. Its **effects** can perhaps be included, or rather accounted for in the data supplied to Abaqus.

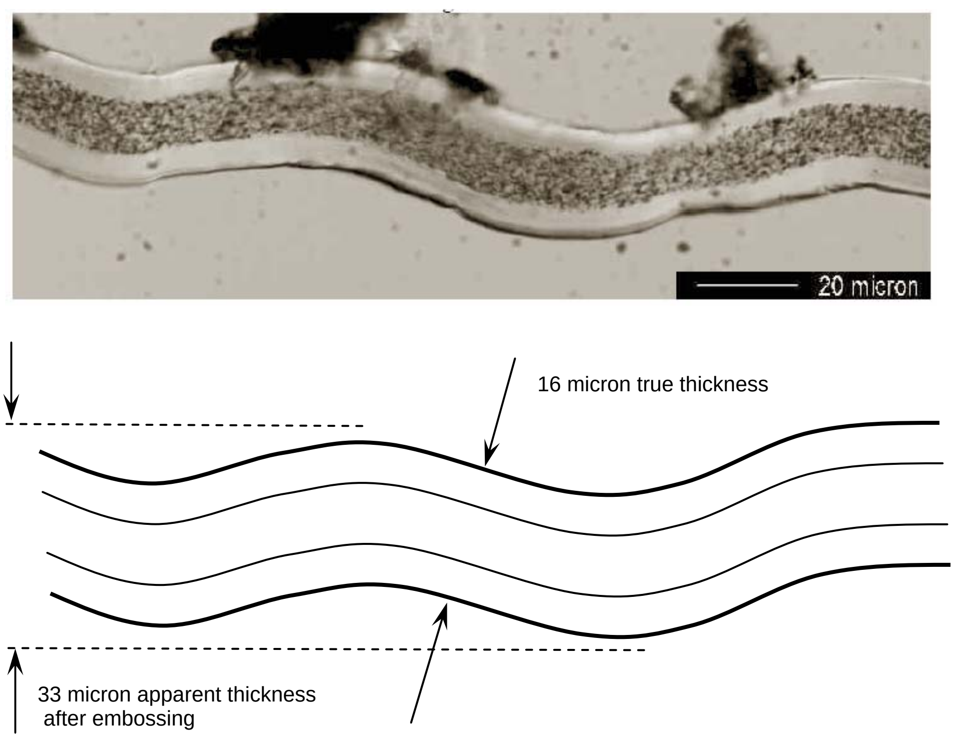

Figure 2 Cross-sectional dimensions of the embossed film.

3. Abaqus analyses

The major steps into which the analysis has been subdivided, is sketched in Figure 3. This sequence follows the natural flowchart of the actual production process for such films, as can be seen with reference to Figure 1.

Some factors which complicate the analysis are:

1. The exact state of internal stress in the thin film (and its distribution) both before and after the embossing process is not known.
2. The material may experience constrained shrinkage on the heating rollers as it approaches the embossing temperature.
3. Theoretical models able to consider alteration of microstructural details in the film are not readily available and in any event would require quite some calibration to obtain meaningful results from.
4. The finer details associated with the manufacturing process are not known; for example what the modulus of the rubber on the backup roll actually is. The rubber modulus will have an effect on the local distribution of pressure onto the thin film while it is being formed into the “bathtub” depression on the engraving roll.

Thus, the approach followed here has been to perform the analysis using relatively-simple models already available within Abaqus, but not so elementary so as to deliver useless results or give poor insight into the mechanisms influencing the problem. The forming process is simply considered to be due to a uniform pressure load applied to the top surface of the heat-softened polymer.

The material model chosen from those available in Abaqus is one that has not been specifically developed to model polymer behavior, but rather that of metals typically showing elastic-plastic behavior. The elastic part of the behavior is taken to be the linear part of the stress-strain curve, while the plastic part is that portion extending past the traditional “yield point”. No loading/unloading tests have been conducted to determine the true amount of recoverable strain. With reference to the material test data curves, the elastic strain would be considered to extend to ca. 10% strain – this is in any case within the region of interest when predicting the stiffness alteration of the film.

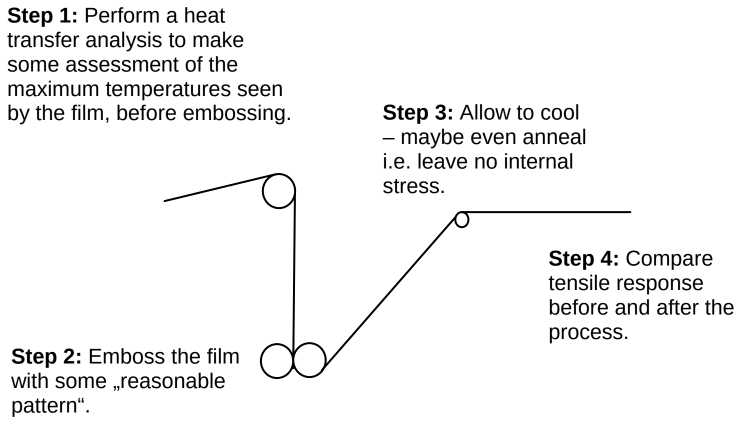

Figure 3 Step sequence of Abaqus analyses.

3.1 Step 1 – Heat Transfer Analysis

The purpose of this analysis is to make some estimate of the maximum temperature experienced by the thin film, before it enters the embossing rollers. Both the deformational properties of the polymer and the total amount of shrinkage on cooling are dependent on this temperature. The film is in contact with the roller for some fraction of the time it would take to cover the whole circumference at the speed of winding. We consider the film and the roller to be flat having no curvature and being infinitely wide along the roller with no gradient "into the paper", thus a 2-D analysis suffices. For constant values of the important heat-transfer coefficients, this problem has a closed-form solution, of course. It was nevertheless solved by FEM - perhaps in anticipation of handling more complicated cases in future.

Heat transfer effects are due to:

1. Heat flow into the sample due to its contacting the roller.
2. Heat flow out of the sample due to radiation and forced convection loss to the surroundings.

There will be some forced convection cooling between the pre-heat roll and the embosser – it is assumed that in practice some radiator banks make up for this loss.

3.2 Step 2 – Embossing Analysis

We examine the deformation of a representative volume element (RVE) of the thin film being "draped" over and into a rigid mesh on the surface of the embossing roller in the "nip" area. The embossing of the film is performed by applying a uniform pressure (in practice applied by a solid surface from the rubber roll, its amplitude increasing and decreasing with time as the roller passes) to the top surface of the film which eventually deforms the surface into a kind of catenary surface. In the absence of more detailed information, this is considered a reasonable approach. The RVE repeats many times over the surface, so we apply symmetrical boundary conditions on all its edges as shown in Figure 4.

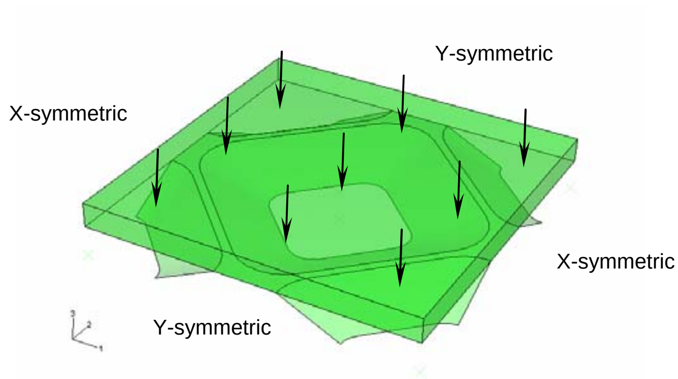

Figure 4 Outline of RVE with suitable boundary conditions in contact with embossing bathtub mesh with uniform pressure applied.

3.3 Step 3 – Cooling Analysis

The cooling analysis is included to account for any thermal shrinkage experienced on addition to the elastic springback at the end of embossing. The cooling down also relaxes the internal forming stresses experienced by the RVE; however the damage introduced into the material is not "healed". No annealing was performed, although this feature does exist in Abaqus. The amount of embossing pressure that is required to be applied is dependent on the degree of orthotropy of the material and how much shrinkage is experienced on cooling. Some iteration was required to bring the final "measured thickness" of the RVE to 33 microns as shown in Figure 2.

3.4 Step 4 – Comparative Tensile Testing Analysis

For these analyses, the force vs. displacement plots from the Abaqus/Explicit analyses are compared for the two cases; a flat unembossed RVE and an embossed one. This analysis is run so that it is representative of a “quasi-static” test; the ratio of kinetic energy to internal energy is kept below 5% during the analysis. The material experiences internal damage as it is extended well into the plastic zone and the failure can be monitored via the scalar damage variable (`DUCTCRT`).

3.5 Parameterized Abaqus input model

Since the shape is fairly regular, one can easily generate the mesh making up the rigid surfaces of the bathtub using suitable *NGEN, *NFILL and *ELGEN commands. The required draft angle is obtained by simply scaling the nodes defining the top “rim of the bathtub” via *NMAP and shifting them by the required depth to the “floor of the bathtub”. The four triangularly-shaped quadrants (NE, SE, SW and NW) around the central bathtub are generated through suitable application of *NCOPY and *ELCOPY commands. The major variables required for parameterized input as seen in Figure 5 for the rigid bathtub mesh generation, are listed in Table 1.

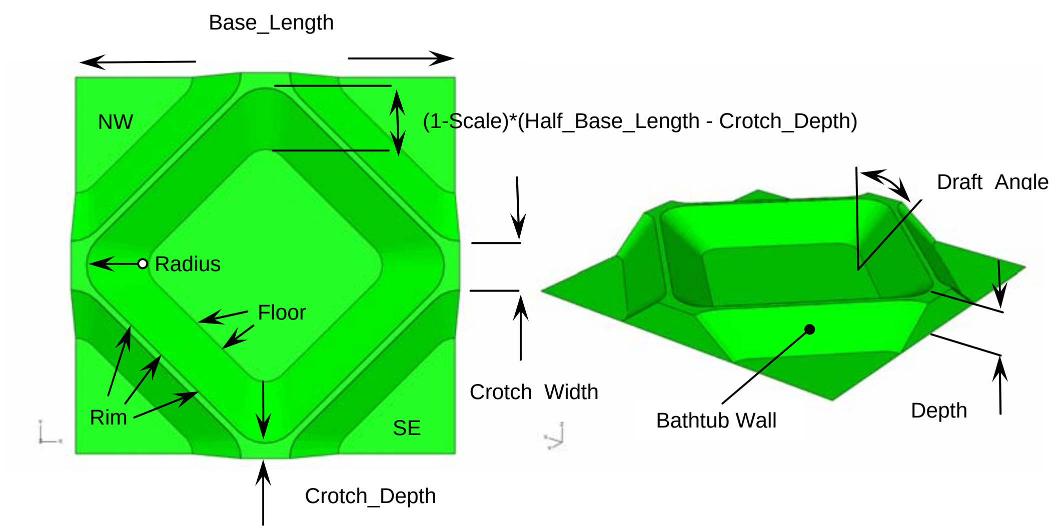

Figure 5 Major `*PARAMETER` references for generating the bathtub mesh.

Table 1 Parameters for generating the mesh

Parameter
Crotch_Depth
Crotch_Width
Base_Length
Scale
Radius
Depth
Draft_Angle = atan((1-Scale)*(Half_Base_Length-Crotch_Depth)/Depth)

4. Analysis material model

The material exhibits both elastic and plastic orthotropy along axes as shown in Figure 6; the curves in Figure 7 clearly show the dependency of mechanical properties on orientation – also in the plastic region. In addition, the material stress vs. strain curves are, in general, functions of temperature and strain rate. Test data, at various temperatures, for the thin film are taken at 0º, 90º and at 45º to the dominant blowing/extrusion axis (machine direction axis). Together with the theoretical material model considerations expounded here, these test data from the testing laboratory are used to define the material to Abaqus, in the form Abaqus expects.

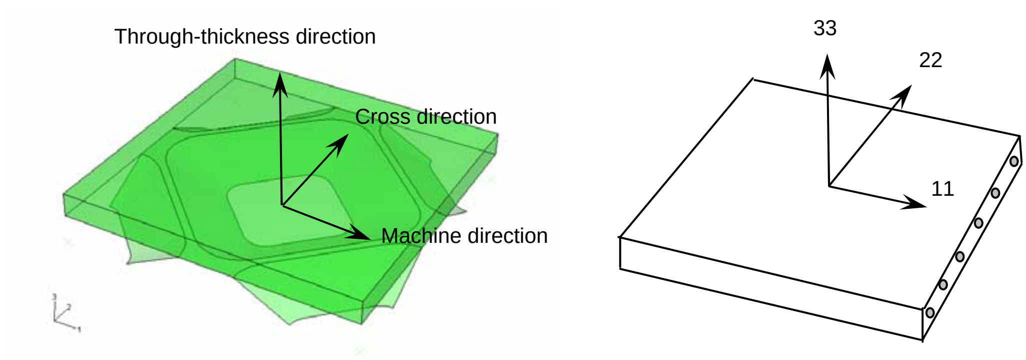

Figure 6 Orthotropic axes definition.

4.1 Elastic and thermal expansion behavior

The in-plane compliance behavior of the film at an angle θ to the machine direction has the following functional relationship [cf. Holmes], which may be used to estimate a realistic value for G_{MC} from a comparison of the test data at 0º, 90º and at 45º to the machine direction axis.

$$\frac{1}{E_{\theta\theta}} = \frac{1}{E_{MD}}\cos^4\theta + \frac{1}{E_{CD}}\sin^4\theta + \left(\frac{-2\nu_{MC}}{E_{MD}} + \frac{1}{G_{MC}}\right)\sin^2\theta\cos^2\theta$$

with,

E_{MD} = Measured elastic modulus along machine direction.

E_{CD} = Measured elastic modulus along cross direction.

G_{MC} = Shear modulus in the plane of film.

ν_{MC} = Poisson´s ratio in the plane of film defined as $\frac{-\varepsilon_{CD}}{\varepsilon_{MD}}$ when loaded along the machine direction with the cross direction being traction free.

From thermodynamic considerations, the constraint $\nu_{MC}^2 < \frac{E_{MD}}{E_{CD}}$ is also relevant.

We need to specify the through-thickness direction properties (cf. Figure 6) for Abaqus in order to have a fully-specified material model. Most of the loading on the thin-film is in-plane and the thickness direction has very little influence on the in-plane behavior in any event, so these properties are estimated. We consider the material to be transversely-isotropic in the plane containing the cross direction and thickness direction i.e. the 22-33 plane and thus

E_{TD} = Estimated elastic modulus along the thickness direction = E_{CD}.

ν_{MT} = Estimated Poisson´s ratio of the film defined as $\frac{-\varepsilon_{TD}}{\varepsilon_{MD}}$ when loaded along the machine direction with the thickness direction being traction free = ν_{MC}

G_{MT} = Estimated transverse shear modulus of the film = G_{MC} .

G_{CT} = Estimated transverse shear modulus of the film is considered to be significantly less than that of G_{MT}, possibly by a factor of half.

The elastic behavior is entered using the Abaqus keyword `*ELASTIC, TYPE = ENGINEERING CONSTANTS` and giving the associated Young´s modulus and Poisson ratio data as a function of temperature, as required. After embossing, the material cools and will generate internal stress owing to its being restrained in the nip area. The thermal expansion behavior is entered using the Abaqus keyword `*EXPANSION, TYPE = ORTHO` and giving the data as a function of temperature, as required.

4.2 Plastic behavior

The extension by Hill to the standard Von Mises plasticity model is able to model the directional dependency of the plastic behavior. The theoretical treatment of this model and axes convention follows those used in the Abaqus manuals. Each yield curve for loading along the other axes is given as a ratio of some reference value, which for our analysis we have taken to be the 11-direction (or machine direction). At first glance, the form of the test data curves in Figure 7 is typical of those for a hyperelastic material or non-linear ***elastic*** material – these data are taken at high temperature. However a hyperelastic material would recover its initial position (zero remaining strain) once the load is removed; the thermoplastic modeled here will not do this and thus the elastic-plastic modeling approach is retained.

The yield function is:

$$f(\sigma) = \sqrt{F(\sigma_{22} - \sigma_{33})^2 + G(\sigma_{33} - \sigma_{11})^2 + H(\sigma_{11} - \sigma_{22})^2 + 2L\sigma_{23}^2 + +2M\sigma_{31}^2 + 2N\sigma_{12}^2}$$

The constants *F,G,H,L,M* and *N* are determined internally by Abaqus from the ratios, R_{ij}, of yield stress functions (they may be temperature dependent, as required) along the different test axes given on the `*POTENTIAL` keyword.

In uniaxial tension

$$R_{ii} = \frac{\sigma_{ii}}{\sigma_0}$$

In shear

$$R_{ij} = \frac{\sigma_{ij}\sqrt{3}}{\sigma_0}$$

The plastic behavior defining the reference yield function along the 11-direction, or machine direction, σ_0, is entered using the Abaqus keyword `*PLASTIC, RATE = <strain_rate>` and giving the associated data as a function of temperature and strain rate as required.

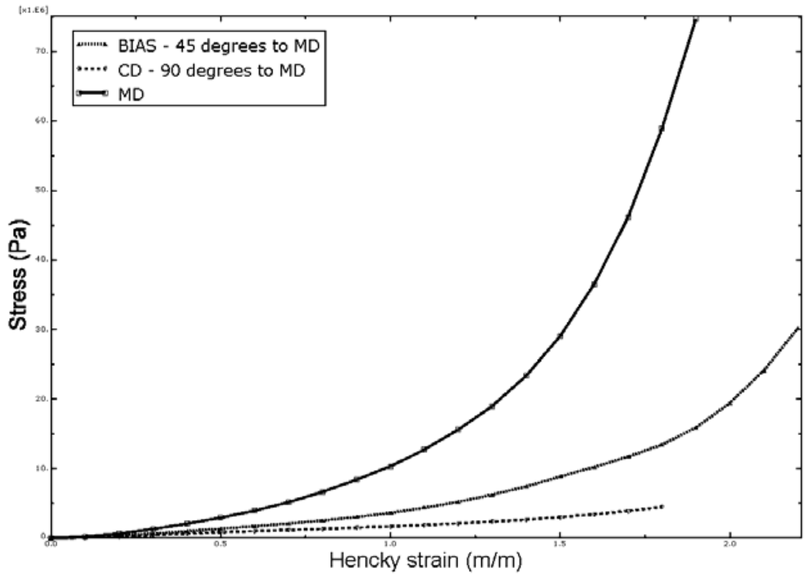

Figure 7 Typical test data - Stress vs. Strain (Hencky) curves illustrating directional dependency.

4.3 Damaging behavior

As the plastic strain increases, internal damage accumulates in the material according to the ductile damage model offered in Abaqus. This model assumes that the equivalent plastic strain, $\overline{\varepsilon}_D^{pl}$ at the onset of damage in a material, is a function of stress triaxiality and strain rate. Thus:

$$\overline{\varepsilon}_D^{pl} = f\left(\eta, \dot{\overline{\varepsilon}}^{pl}\right)$$

where

$\eta = \dfrac{-p}{q}$, an index denoting the stress triaxiality

$\dot{\overline{\varepsilon}}^{pl}$ = Equivalent plastic strain rate.

The criterion for damage initiation is when an internal material state variable reaches the value unity, as given by the following equation:

$$\varpi_D = \int \frac{\delta \bar{\varepsilon}_{pl}}{f\left(\eta, \dot{\bar{\varepsilon}}^{pl}\right)} = 1$$

This is a monotonically increasing function with strain – the material thus never heals upon reversal of the strain state.

The model is described Abaqus keyword `*DAMAGE INITIATION` keyword. Once damaged, the material follows a response given by a dependence on the total displacement at complete failure (entered on the `*DAMAGE EVOLUTION` card in Abaqus).

4.4 Calibrating the Material Model

It is not possible to perfectly calibrate the material model in all directions, for all temperatures – thus a compromise has to be settled on. The machine direction at room temperature is the most important to get right since it plays a major role in the stiffness of the film. The orthotropic Von Mises model is unable to represent any behavior along the other axes which is different in **character** to that along the machine direction because in essence these are all scaled versions of the baseline behavior. For example, along the cross direction, the material shows the typical "kink" (which is typical for these extruded films, due to internal re-arrangement of the polymer ligaments) in the stress vs. strain curve as shown in Figure 8 and this detail cannot be captured independently from that occurring along the machine direction. The tailoring of the failure parameters is extremely difficult to perform, especially so for a material which is significantly outside the range of "normal metal plasticity" – there is, for example, some significant localization behavior in the mesh used for material calibration. Since the exact prediction of this failure point was not considered important (only as aid to show how the embossing pattern leaves a damaged imprint in the film) this was not pursued to any degree more than necessary to get a reasonably stable analysis.

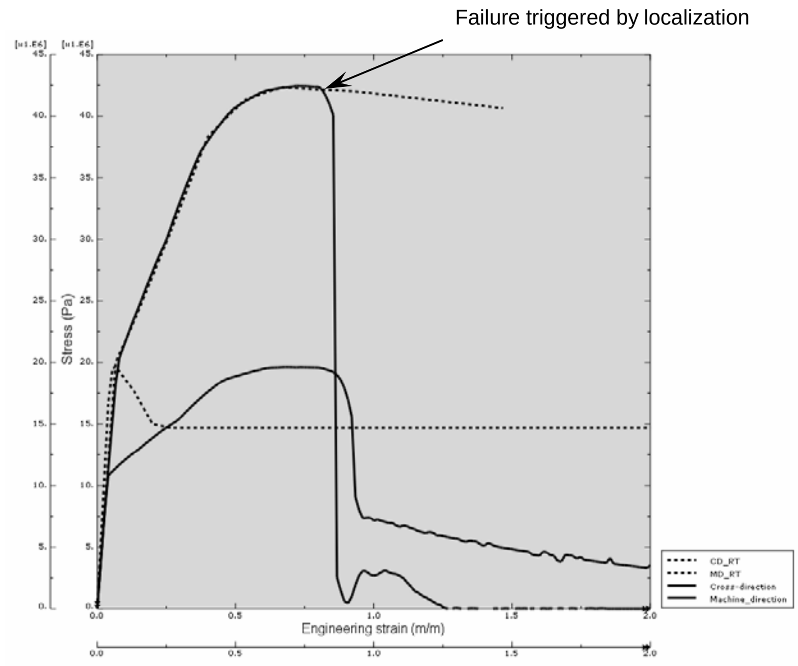

Figure 8 Calibration curve showing excellent agreement along machine direction at room temperature and compromise calibration curve along cross direction.

5. RESULTS

5.1 Step 1 – Heat Transfer Analysis

As was intuitively to be expected, the thin film reaches steady state temperature conditions very quickly and may be considered to be uniformly-heated throughout.

5.2 Step 2&3 – Embossing and Cooling Analysis

During embossing, the material experiences three phases of deformation viz. a bending dominated phase, a stretching dominated phase and finally some elastic springback as it leaves the forming bathtub. These phases are sketched in the graphic in Figure 9 – the apparent thickness is computed through differencing the changes in displacement position between suitably-chosen mesh points on opposite sides of the thin film. Initially there is no displacement difference (they are both zero) and the curve starts at zero, but then eventually asymptotes to the apparent thickness after drape forming. There is an additional change in dimensions caused by thermal expansion – shrinkage in this case, which is not shown on the graphic; it is similar to the elastic springback step.

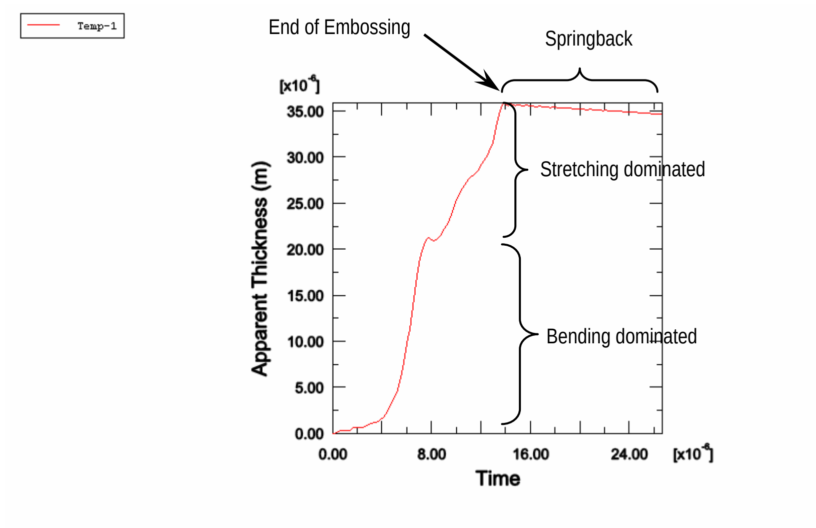

Figure 9 Apparent thickness of film vs. time(s) during drape embossing.

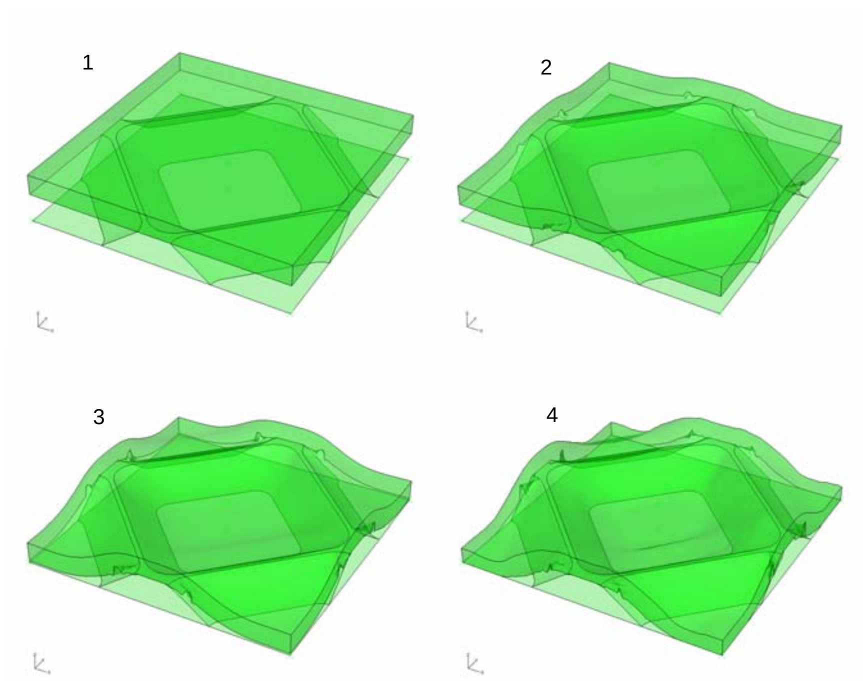

Figure 10 Illustration of typical stages in drape forming process of the RVE.

5.3 Step 4 – Comparative Tensile Testing Analysis

The comparative stiffness before and after embossing is illustrated in Figure 11 for the 2 different directions and 2 different states of the film. It should be borne in mind that these results come from different batches of the material – the material data used for calibrating the analysis material model is not from the same batch as that used to generate the experimental curves in Figure 11. The analysis shows a surprisingly good ability to predict a change of stiffness in the **machine direction** from the flat film state to when embossed, considering the complexity of the material. In order to generate these points from the analysis output, the apparent thickness for each type of film (33 microns and 16 microns) has been used to compute the cross-sectional stress from the forces applied in the analysis. The simplified approach of simply forming the film via a pressure load on the top surface has caused a more convoluted shape in the cross direction than in the machine direction – this illustration is not shown here. This has left the film to be relatively more flexible in this cross direction and immediately shows up the relative importance of the geometric effect vs. the material orthotropic effect for even these small strains.

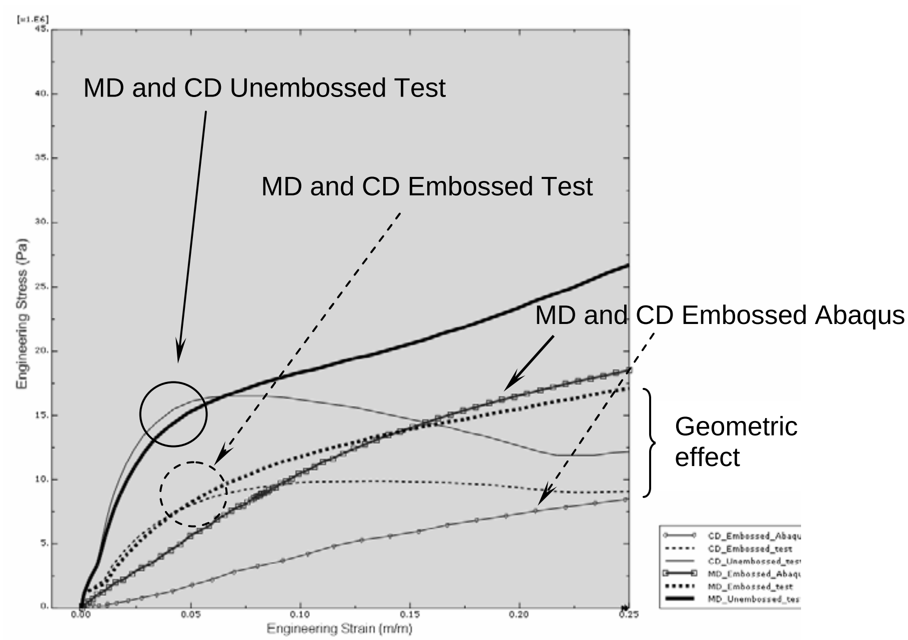

Figure 11 Comparison between simulation and experimental stiffness.

A point to note is that up to the moderate levels of strain attained in the graphic in Figure 11, the basic unembossed film is surprisingly isotropic in its behavior; only after ca. 7.5%-10% strain does this start to change as the material starts to yield. This experimental behavior is consistent with the test data from the batch used to generate the elastic data cards for the film at room temperature.

6. CONCLUSIONS

It is possible using a fairly simple metal plasticity model in Abaqus to predict the stiffness change due to embossing of the thin film. If predicting only the stiffness change for varying shapes of embossing pattern is the goal, then one may consider this materials particular behaviour to be isotropic rather than assuming it to be orthotropic as has been done here; this will reduce dramatically the experimental support required.

The ultimate load carrying capacity is much more difficult to predict, even using fairly sophisticated extensions to this material model. There is probably no sense in performing such an analysis, using the most sophisticated extensions available to a Von Mises model, since the model is fundamentally unable to account for many of the complicating factors in such materials at higher strains. If this were to be a requirement in future, significant effort would need to be invested to develop such a material model. This effort would constitute both significant theoretical and experimental work, possibly resulting in the writing of a `FORTRAN VUMAT` subroutine extension to Abaqus.

7. References

1. Holmes M. and Just D.J., ***GRP in Structural Engineering***, Applied Science Publishers, ISBN 0-85334-232-6

2. Kamal M.R., Haber A. and Ryan M.E., "An Engineering Study of the Film Embossing Process", Polymer Engineering and Science, Mid-August, 1985, Vol. 25 Nr. 11.

3. Kamal M.R., Haber A. and Song Li, "The Effect of Processing Conditions on the Microstructure of Embossed Polyethylene Films", Polymer Engineering and Science, Mid-February, 1988, Vol. 28 Nr. 3.

4. Kamal M.R., Haber A., "Experimental Analysis of the Thermoplastic Film Embossing Process", Advances in Polymer Technology, Vol. 11 Nr. 3, 159-180 (1992), John Wiley and Sons.

5. Nagarajan P. et al., "Rubber-Assisted Embossing Process", School of Polymer, Textile and Fibre Engineering, Georgia Institute of Technology, Atlanta, Georgia (30332)